50 m waters of the BOB are an indication of the oligotrophic nature of the water that eventually leads to very low biological production.

1. Banse, K., *Deep-Sea Res.*, 1987, **34**, 713–723.
2. Bauer, S., Hitchcock, G. L. and Olson, D. B., *Deep-Sea Res.*, 1991, **38**, 531–533.
3. Shetye, S. R., Shenoi, S. S. C., Gouveia, A. D., Michael, G. S., Sundar, D. and Nampoothiri, G., *Continent. Shelf Res.*, 1991, **11**, 1397–1408.
4. Prasanna Kumar, S. and Prasad, T. G., *Curr. Sci.*, 1996, **71**, 834–841.
5. Prasanna Kumar, S. *et al.*, *Deep-Sea Res. II*, 2001, 1115–1126.
6. Barber, R. T. *et al.*, *Deep-Sea Res. II*, 2001, **48**, 1127–1172.
7. Madhupratap, M., Prasanna Kumar, S., Bhattathiri, P. M. A., Dileep Kumar, M., Reghu Kumar, S., Nair, K. K. C. and Ramaiah, N., *Nature*, 1996, **384**, 549–552.
8. Bhattathiri, P. M. A., Aditi Pant, Surekha Sawant, Gauns, M., Matondkar, S. G. P. and Mohanraju, R., *Curr. Sci.*, 1996, **71**, 857–862.
9. Veldhuis, M. J. W., Kraay, G. W., Van Bleijswijk, J. D. I. and Baars, M. A., *Deep-Sea Res. I*, 1997, **44**, 425–449.
10. Ramage, C. S., Climate of the Indian Ocean north of 35°S. In *World Survey of Climatology, Climates of the Oceans* (ed. Van Loon, H.), Elsevier, Amsterdam, 1984, vol. 15, pp. 603–659.
11. Varkey, M. J., Murthy, V. S. N. and Suryanarayana, A., Physical Oceanography of Bay of Bengal, In *Oceanography and Marine Biology: An Annual Review*, UCL Press, 1996, vol. 34, pp. 1–70.
12. Radhakrishna, K., *Indian J. Mar. Sci.*, 1978, **7**, 58–60.
13. Radhakrishna, K., *Indian J. Mar. Sci.*, 1978, **7**, 94–98.
14. Devassy, V. P., Bhattathiri, P. M. A. and Radhakrishna, K., *Mahasagar*, 1983, **16**, 443–447.
15. Bhattathiri, P. M. A., Devassy, V. P. and Radhakrishna, K., *Mahasagar*, 1980, **13**, 315–323.
16. Madhupratap, M. *et al.*, *Deep-Sea Res. II*, 2002, **50**, 881–896.
17. Gomes, H. R., Goes, J. I. and Saino, T., *Continent. Shelf Res.*, 2000, **20**, 293–311.
18. Strickland, J. D. H. and Parsons, T. R., In *A Practical Handbook of Sea Water Analysis*, Bull. Fish. Res. Board Can., 1972, 2nd edn, vol. 167, p. 310.
19. UNESCO, Protocols for the Joint Global Ocean Flux Study, Manual and Guides, 1994, vol. 29, p. 170.
20. Gifford, D. J. and Caron, D. A., ICES, *Zooplankton Methodology Manual*, Academic Press, New York, 2000.
21. Hastenrath, S. and Lamb, P. J., *Climatic Atlas of the Indian Ocean, Part. 1: Surface Climatic and Atmospheric Circulation*, The University of Wisconsin Press, Wisconsin, 1979, p. 104.
22. Shetye, S. R. *et al.*, *J. Geophys. Res.*, 1996, **101**, 14011–14025.
23. Han, W., McCreary, J. P. and Kohler, K. E., *J. Geophys. Res.*, 2001, **106**, 6895–6916.
24. Pankajakshan, T., Gopalakrishna, V. V., Muraleedharan, P. M., Reddy, G. V., Nilesh, A. and Shenoi, S., *Deep-Sea Res. I*, 2002, **49**, 1801–1818.
25. Rao, C. K., Naqvi, S. W. A., Kumar, M. D., Varaprasad, S. J. D., Jayakumar, D. A., George, M. D. and Singbal, S. Y. S., *Mar. Chem.*, 1994, **47**, 279–290.

ACKNOWLEDGEMENTS. This work was carried out under the Marine Research–Living Resources (MR–LR) Assessment programme with financial assistance from the DOD, New Delhi. We thank the Director, National Institute of Oceanography (NIO), Goa for the facilities provided. We also thank NASA, USA and Dr T. Suresh, NIO, Goa for the Sea WiFS chlorophyll data. R.J. and P.A.M. thank CSIR, New Delhi for financial support.

Received 12 November 2003; revised accepted 26 May 2004

Low period variability in Tropical Rainfall Measuring Mission Microwave Imager measured sea surface temperature over the Bay of Bengal during summer monsoon

Anant Parekh, Abhijit Sarkar*, Shivani Shah and M. S. Narayanan

Meteorology and Oceanography Group, Space Applications Centre, Ahmedabad 380 015, India

Sea surface temperature measured by the Tropical Rainfall Measuring Mission Microwave Imager (TMI) over the Bay of Bengal during monsoon was found to exhibit a low-period intra-seasonal mode of 8–16 days, in addition to the 30–60 days mode. This unique feature is attributed to the coherent response of the top fresh-water layer, formed due to high precipitation and river run-off, to synoptic atmospheric monsoon processes. These results were obtained through Fourier, Morlet wavelet and time series analyses applied on TMI and buoy data of June–September during 1998–2001.

SEA surface temperature (SST) displays variability over a wide range of space- and time-scales. Over the tropical oceans, SST variability has been shown to be associated with the oscillations of a variety of weather patterns. The most pronounced oscillations in SST are known to occur over the Bay of Bengal (BoB) besides the equatorial western Pacific Ocean[1]. The recent observations by space-borne microwave sensors of SST in the tropical oceans under the influence of cloudiness and precipitation, have further enriched the understanding of its variabilities.

Variability in meteorological and oceanographic parameters over the monsoon regions of north Indian Ocean, consisting of the Arabian Sea (AS) and the BoB, continues to be the focus of active research on monsoon variability[2]. Yasunari[3], and Sikka and Gadgil[4] found two dominant periodicities of around 40 and 15 days in the fluctuations of cloudiness over the northern Indian Ocean (IO) during summer monsoon. Fluctuations of the 40 day period were shown to represent the marked northward movement of the cloudiness from the equatorial zone to the mid-latitudes, while the 15-day period mode seems to correspond with the movement of equatorial monsoonal disturbances. Murakami[5], and Krishnamurti and Bhalme[6] have also noted a period of around two weeks for the alteration between active and inactive phases of monsoon for near-normal rainfall years. In a recent study based on the spectral analysis of observations made during the Bay of Bengal Monsoon Experiment (BOBMEX), Hareeshkumar *et al.*[7] found prominent peaks at around 10.6 days in the *V*-

*For correspondence. (e-mail: sarkar_abhi2000@yahoo.com)

component of ocean surface wind, U-component of ocean current, air temperature as well as SST (measured at the depth of a few centimetres).

The present study was carried out with simultaneous, instantaneous and quality-checked SST observations made by the microwave radiometer on-board the Tropical Rainfall Measuring Mission (TRMM) satellite and IO buoys during the summer monsoon months (viz. June–September) during 1998–2001. The study aims to explore the existence of a low period variability in the skin SST (as observed by the microwave radiometer) in the BoB and the AS. The study also explores the nature of variabilitiy in SST measurements at a depth (IO buoy measurements are made at a depth of 3 m). In order to bring out the SST variability in both time and frequency domains, Morlet wavelet transform in addition to conventional Fourier transform was applied on the time series observations.

TRMM, a joint NASA–NASDA mission has on-board the microwave radiometer TMI[8] (TRMM Microwave Imager). The TMI has a full suite of channels ranging from 10.7 to 85 GHz, and represents the first satellite sensor that is capable of accurate measurements of SST through clouds. The rain-sensitive channels on-board TMI are used to detect rain in the radiometer field-of-view. When rain is detected, SST retrieval is discarded[9]. Because of its frequent repeat, non sun-synchronous orbit, the TMI SST dataset provides an unprecedented look at the IO basin scale SST variability under atmospheric convection conditions[10]. By virtue of its low-altitude orbit (~ 350 km), TMI has improved ground resolution (25 km × 25 km) in comparison to other satellite missions with similar microwave sensors. For this study, daily gridded Version 3 TMI SST data (available on-line through remote sensing systems at http://www.ssmi.com/) were used.

The *in situ* SST data are obtained from National Institute of Ocean Technology (NIOT), Department of Ocean Development, India. Several deep-sea and shallow-water moored buoys have been functional in the north IO since 1997 under the National Data Buoy Programme[11]. Five deep-sea buoys were operated during 1997–2001; no single buoy, unfortunately, acquired data over the entire period of this study. The SST sensor on the NIOT buoy is installed at ~ 3 m below the sea surface. The reported SST is the average value of 600 samples (measurements acquired over 10 min with sampling speed of 1 sample/s) every 3 h. The stated accuracy of SST sensor is ± 0.1°C, with 0.01°C resolution.

Two representative IO data buoys (DS1 in the AS and DS3 in the BoB) were selected for this study. DS1 is located at 15.5°N lat/69.3°E long, and DS3 at 13.0°N lat/87.0°E long during the years 1998 and 1999 and at 12.2°N lat/90.8°E long (central BoB) during 2000 and 2001. These are shown in Figure 1, along with information on major river run-offs over the north IO basin (the arrow thickness approximately indicating the run-off magnitudes during summer monsoons)[12]. Also shown in Figure 1 are the daily average rainfall contours over the north IO during the summer monsoon period[13].

The main focus of the present study was on the result obtained through Fourier and wavelet analysis on SST anomaly (with respect to its seasonal mean) time-series data of buoy and TMI within the spatial window of ± 75 km with respect to the buoy location. This was preceded by time series and statistical correlation analyses of these two datasets consisting of the original instantaneous observations. The impact of wind on the variations in the temperature difference between the buoy and the TMI was also assessed using the three-day running mean time-series data (not shown here).

For carrying out a comparison of spectral characteristics between the TMI-derived SST values and those measured by the buoys in the BoB and in the AS, all TMI three-day running mean data within the selected spatial window around the buoy locations were averaged and paired with the corresponding three-day means of buoy data (by averaging the relevant 3 h measurements). Three-day running mean data, being free from undesirable gaps and jumps, were found ideal for our spectral analysis. Fourier power spectrum analysis was carried out with this dataset. Figure 2 *a* and *b* shows the power spectrum for the AS and BoB respectively. Continuous lines are for satellite measurements and dotted lines are for buoy measurements.

Finally, for studying the dominant modes of localized signals such as our SST time series, we have adopted the Morlet wavelet analysis. The wavelet analysis[14,15] enables determination of the amplitude and phase of each harmonic, and thus allows detailed analysis of time-dependent signal characteristics.

The wavelet transform $W_n(s)$ for a time series X_n, with $n = 0, 1, 2, \ldots N-1$ and equal temporal spacing δt, is usually defined as the convolution of X_n with a scaled and translated version of $\psi(\eta)$:

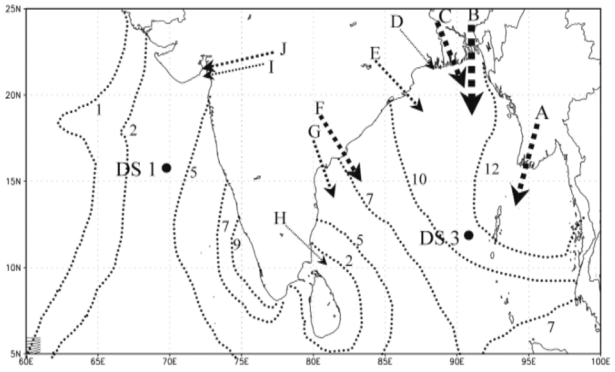

Figure 1. North Indian Ocean basin with the moored buoy (DS1 and DS3) locations. Contours show the daily averaged rainfall (mm/day) and the arrows indicate run-offs of the major rivers in the region during the summer monsoon period, viz. A, Irrawaddy; B, Brahmaputra; C, Ganga; D, Damodar; E, Mahanadi; F, Godawari; G, Krishna; H, Cauvery; I, Tapi and J, Narmada. Arrow thickness roughly indicates run-off magnitudes for summer monsoon.

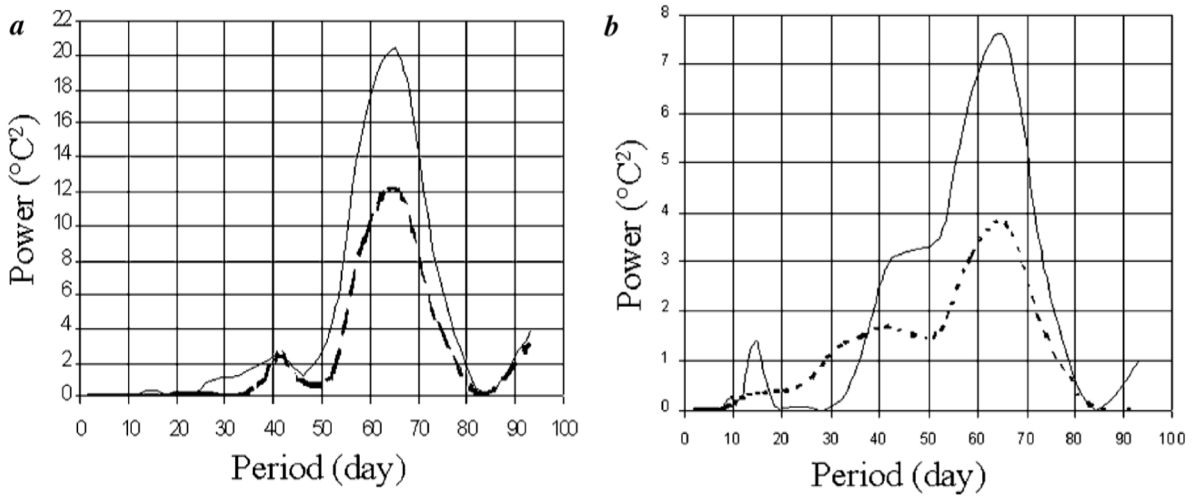

Figure 2. Fourier power spectrum analysis of SST anomaly for (***a***) AS (at DS1 location in 1998); and (***b***) BoB (at DS3 location in 2000). Continuous lines are for TMI and dotted lines for buoy measurements.

$$W_n(s) = \sum_{n'=0}^{N-1} X_n \psi^* \left[\frac{(n'-n)\delta t}{s} \right].$$

Here, $\psi(\eta)$ defines the wavelet function and the asterisk indicates its complex conjugate; s is the wavelet scale. Our analysis is performed using the Morlet wavelet function, a plane wave modulated by a Gaussian:

$$\psi(\eta) = \pi^{-1/4} \exp(i\omega\eta) \exp(-\eta^2/2),$$

where η and ω are the non-dimensional time and frequency respectively. The Morlet wavelet function $\psi(\eta)$ being complex, allows detection of both the time-dependent amplitude $|W_n(s)|$ and the phase $\tan^{-1}[I\{W_n(s)\}/R\{W_n(s)\}]$. $I\{W_n(s)\}$ and $R\{W_n(s)\}$ are the imaginary and real parts of our wavelet transform and the wavelet power spectrum is simply $|W_n(s)|^2$. To determine what portion of the signal is significant, the approach suggested by Torrence and Compo[15], in which the time series is modelled as red noise, is used. If a point of the wavelet spectrum is greater than 95% of the chi-square distribution curve for this mean spectrum, the signal is significant. We have used this method in analysing all our results described below. Errors get introduced in the beginning and at the end of the wavelet power spectra due to the finite length of the time series, which are reflected in the cone of influence (cross-hatched regions), of the wavelet power spectra (Figures 3–6).

These exercises were carried out with monsoon-period data of all the four years' (1998–2001) TMI data and available buoy data (1998, 1999 and 2001 at DS1 and 2000 at DS3). As data gaps during 1998 at DS1 and during 2000 at DS3 are minimal, results for these cases have been presented here.

The range of TMI SST as seen in our time series (viz. 26–31°C in the AS and 27–31°C in the BoB) agrees reasonably well with the SST-climatology for the monsoon months (26–29°C in the AS and 28–29°C in the BoB), generated with ship measurements[16]. The time series of instantaneous TMI-sensed skin (i.e. the top thin layer of a few millimetre thickness[17] SST values appears highly fluctuating against the background of relatively smooth variations of subsurface temperature measurements of the buoy. The fact that the TMI SST manifests such fluctuations can be attributed to the response of the oceanic top thin layer to changes in wind speed, humidity and fluxes[18,19]. It is also observed that the TMI-buoy temperature difference of significant magnitude (greater than 0.5°C) persisted in at least five occasions, each lasting for four to eight days during the study period. Thus, a strong thermal stratification in the topmost layer was found to exist in the BoB even in the presence of high winds (higher than 6 m/s). Out of 128 days of the study period, 120 days had winds greater than 6 m/s.

Comparison exercise, carried out with four years' (1998–2001) monsoon months' data of SST derived from TMI, with those measured by IO buoys shows a root mean square difference of about 0.65°C for instantaneous and 0.59°C for three-day running mean data. The results for the instantaneous measurements have not been reported earlier. The value for three-day running mean data is consistent with those by Senan *et al.*[20] in the Indian seas (0.60°C) and by Wentz[9], obtained with one-day averaged data in other oceans (0.5–0.7°C). Chelton *et al.*[21] had obtained a better result with TAO buoy array with three-day running mean data (~ 0.41°C).

The sub-seasonal scale oscillations of 30–60 days (to be more precise, 30–80 days in our results) in SST is prominently seen in the Fourier power spectra of the AS

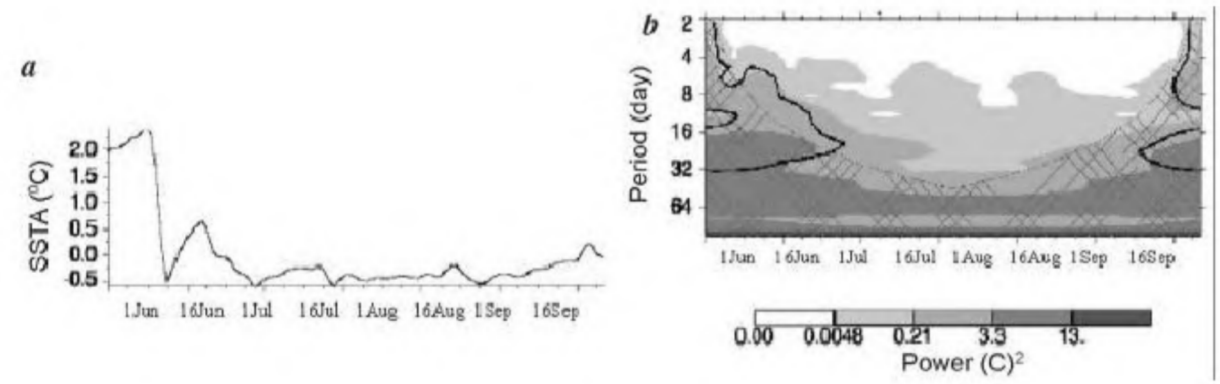

Figure 3. (*a*) Time series, and (*b*) wavelet power spectrum for SST anomaly from AS buoy (DS1) observations between 26 May and 30 September 1998.

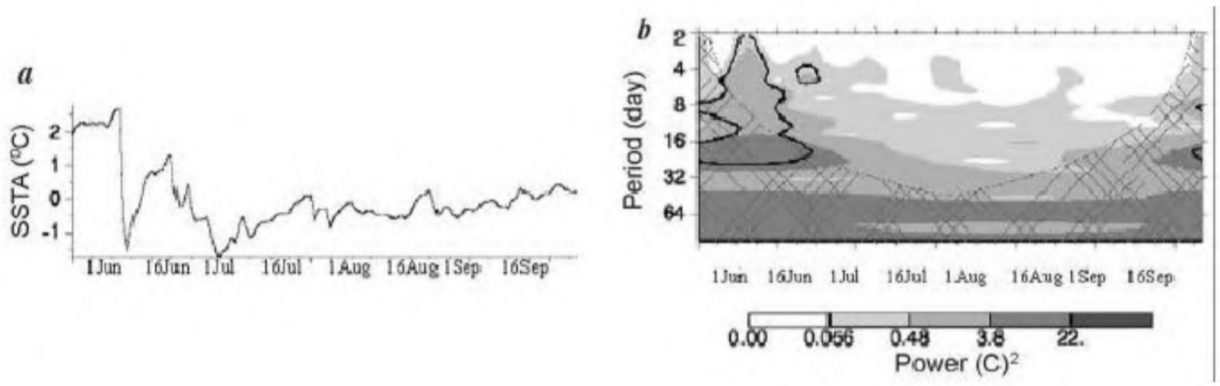

Figure 4. (*a*) Time series, and (*b*) wavelet power spectrum for SST anomaly over AS (at DS1 location) with TMI observations between 26 May and 30 September 1998.

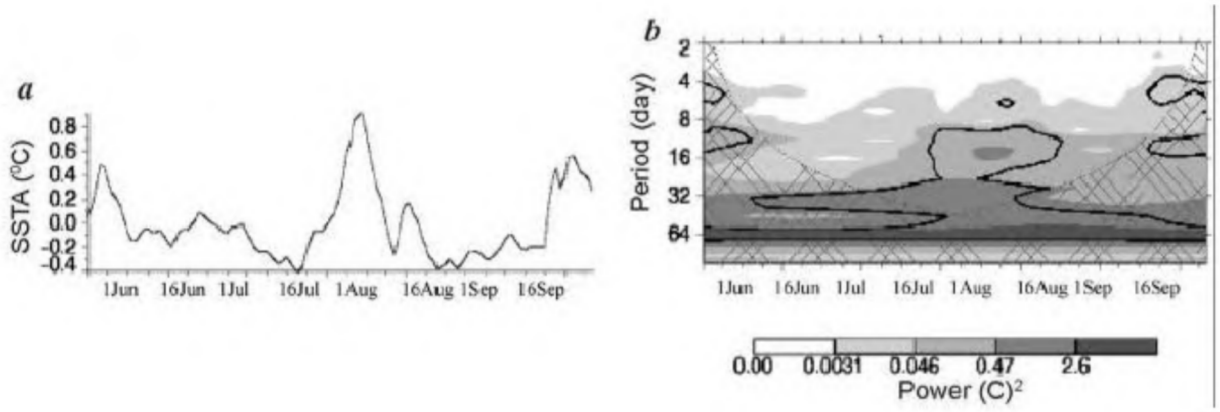

Figure 5. (*a*) Time series, and (*b*) wavelet power spectrum for SST anomaly from BoB buoy (DS3) observations between 26 May and 30 September 2000.

(Figure 2 *a*) and the BoB (Figure 2 *b*), corroborating the results of Sengupta and Ravichandran[22], Sengupta *et al.*[23] and Vecchi and Harrison[24]. The power magnitudes for the buoy measurements are somewhat suppressed with respect to those of satellite measurements (see Figure 2).

What is however more significant is that our TMI Fourier and wavelet results for BoB reveal additional oscillations of 8–16 days period (continuous line in Figure 2 *b* and dark contours with confidence level of 95% and above in Figure 6 *b* for wavelet power spectra). These low period

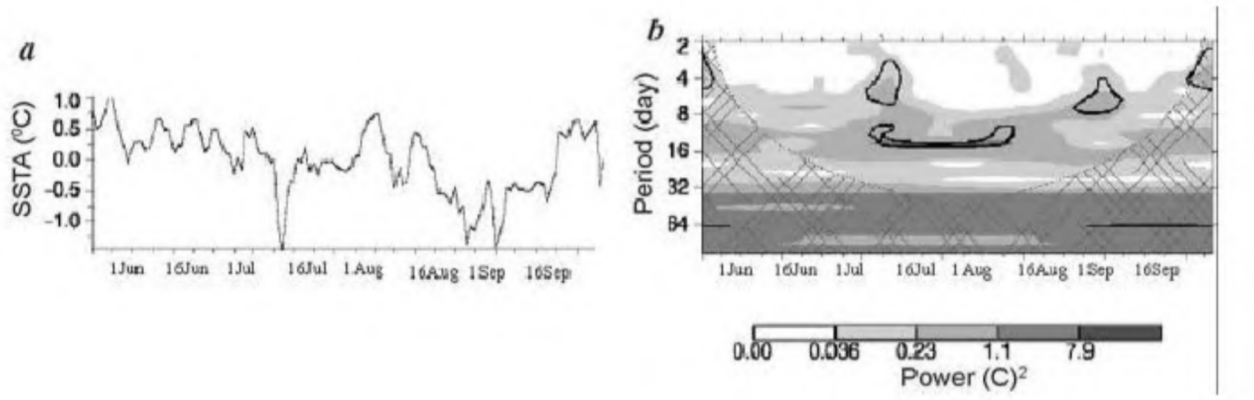

Figure 6. (*a*) Time series, and (*b*) wavelet power spectrum for SST anomaly over BoB (at DS3 location) with TMI observations between 26 May and 30 September 2000.

oscillations are known to exist for synoptic-scale atmospheric phenomena over the monsoonal regions[3–5]. Such synoptic-scale disturbances are known to be associated with the convection processes over the BoB[4] and one would expect a reflection of this signal in the skin SST (as seen in our results for TMI SST over the BoB). SST measured at a depth of 3 m (by buoy), however, does not show low period oscillations (Figure 2 *b*). Wavelet analysis (Figure 5 *b*) shows low period oscillations, but of much lower amplitude (than seen in the satellite data). Besides, it is short-lived (1–16 August 2000, covering only one cycle).

This could be due to strong near-surface stratification in the BoB, formed by large inflow of freshwater because of heavy precipitation (~ 11 mm/day around DS3 buoy location) and large river run-offs in this basin[25]. The run-offs of major BoB rivers, viz. the Brahmaputra, Ganges and Irrawaddy, are as high as 252.9×10^9, 184.7×10^9 and 217.2×10^9 m^3 respectively, for the summer monsoon[12]. This is reflected qualitatively in Figure 1. Formation of this top thin layer, also known as the 'low salinity cap'[26], leads to weakening of the coupling between the skin and sub-surface temperature variabilities.

The corresponding precipitation and river run-off magnitudes being meagre in the AS (~ 4 mm/day around DS1 buoy location), formation of any freshwater layer, which could result in upper-layer stratification, does not take place. Besides, low period convective systems are less in the AS than in the BoB. This explains why the features described above for the BoB are not observed in the TMI results for the AS (Figures 2 *a*, 3 and 4).

SST of the BoB measured during monsoon months by the microwave radiometer aboard the TRMM satellite shows the presence of low period oscillations of 8–16 days, in addition to the commonly known 30–60 days mode. It is conjectured that this is a manifestation of response of the top freshwater layer of the Bay to the synoptic scale oscillations corresponding to the active and break periods of the monsoon. Such low period oscillations are not found in the *in situ* SST data at 3 m depth, presumably due to strong stratification. Observations of low period modes in the surface data reported during BOBMEX programme confirm our results.

1. Krishnamurti, T. N., Oosterhof, D. K. and Mehta, A. V., *J. Atmos. Sci.*, 1988, **45**, 1304–1322.
2. Gadgil, S., *Earth Planet. Sci.*, 2003, **31**, 429–467.
3. Yasunari, T., *J. Meteorol. Soc. Jpn.*, 1979, **57**, 227–242.
4. Sikka, D. R. and Gadgil, S., *Mon. Weather Rev.*, 1980, **108**, 1840–1853.
5. Murakami, M., *J. Meteorol. Soc. Jpn.*, 1976, **54**, 15–31.
6. Krishnamurti, T. N. and Bhalme, H. N., *J. Atmos. Sci.*, 1976, **33**, 1937–1954.
7. Hareeshkumar, P. V., Prasadarao, C. V. K., Swain, J. and Madhusudanan, P., *Curr. Sci.*, 2001, **80**, 786–790.
8. Kummerow, C., Barnes, W., Kozu, T., Shive, J. and Simpson, J., *JAOT*, 1998, **15**, 809–817.
9. Wentz, F. J., Geneteman, C., Smith, D. and Chelton, D., *Science*, 2000, **288**, 847–850.
10. Harrison, D. E. and Vecchi, G. A., *Geophys. Res. Lett.*, 2001, **28**, 3717–3720.
11. Premkumar, K., Ravichandran, M., Kalsi, S. R., Sengupta, D. and Sulochana, G., *Curr. Sci.*, 2000, **78**, 323–330.
12. Varkey, M. J., Murty, V. S. N. and Suryanarayana, A., *Oceanogr. Mar. Biol., Annu. Rev.*, 1996, **34**, 1–70.
13. Grabl, H., Jost, V., Ramesh Kumar, Schulz, J., Bauer, P. and Schlussel, P., Report no. 312, Max Planck Institute for Meteorologie, 2000.
14. Farge, M., *Annu. Rev. Fluid Mech.*, 1992, **24**, 395–457.
15. Torrence, C. and Compo, G. P., *Bull. Am. Meteorol. Soc.*, 1998, **79**, 61–78.
16. Rao, R. R., Molinari, R. L. and Festa, J. F., Surface meteorological and near surface oceanographic atlas of the tropical Indian Ocean. NOAA Tech. Mem. ERL AOML, 69, 1991.
17. Donlon, C. J., Minnet, P. J., Gentemann, C., Nightingale, T. J., Barton, I. J., Ward, B. and Murray, M. J., *J. Climate*, 2002, **15**, 353–369.
18. Wick, G. A., Emery, W. J., Kantha, L. H. and Schlussel, P., *J. Phys. Oceanogr.*, 1996, **26**, 1969–1988.
19. Schlussel, P., Emery, W. J., Grassl, H. and Mammen, T., *J. Geophys. Res.*, 1990, **95**, 13341–13356.

20. Senan, R., Anitha, D. S. and Sengupta, D., CAOS Rep. 2001 AS1, 2001.
21. Chelton, D. B. *et al.*, *J. Climate*, 2001, **14**, 1479–1498.
22. Sengupta, D. and Ravichandran, M., *Geophys. Res. Lett.*, 2001, **28**, 2033–2036.
23. Sengupta, D., Goswami, B. N. and Senan, R., *Geophys. Res. Lett.*, 2001, **28**, 4127–4130.
24. Vecchi, G. A. and Harrison, D. E., *J. Climate*, 2002, **15**, 1485–1493.
25. Shenoi, S. S. C., Shankar, D. and Shetye, S. R., *J. Geophys. Res.*, 2002, **107**, 1–14.
26. Rao, S. A., Gopalakrishna, V. V., Satish, R., Shetye, S. R. and Yamagata, T., *Geophys. Res. Lett.*, 2002, **29**, 1–4.

ACKNOWLEDGEMENTS. We thank Dr K. N. Shankara and Dr Pranav Desai for encouragement. We also thank Drs D. Sengupta, R. R. Rao and V. Sathyamurthy for stimulating discussions and Dr K. Satheesan, Mr Vihang Bhatt, Mr S. H. Rahman for help in data analysis. This work is supported by the Department of Ocean Development, New Delhi. We thank the Remote Sensing Systems, USA for providing TMI data on their website. The wavelet software was accessed from URL: paos.colorado.edu/research/wavelets.

Received 20 January 2004; revised accepted 29 May 2004

Effect of pre-sowing treatment on seed germination and seedling vigour in *Angelica glauca*, a threatened medicinal herb

Jitendra S. Butola and Hemant K. Badola*

G.B. Pant Institute of Himalayan Environment and Development, Himachal Unit, Mohal-Kullu 175 126, India

***Angelica glauca* (Apiaceae), endemic to the Himalayas, is an endangered medicinal plant for which *ex situ* cultivation has been recommended as a conservation strategy. However, seeds of this species show poor germination. Among the 14 pre-sowing treatments, KNO_3 (150 mM) and $NaHClO_3$ (30 min) significantly stimulated seed germination and reduced mean germination time under both laboratory and nursery trials, as well as developed seedling vigour under nursery conditions.**

DISTRIBUTED from temperate to alpine belts of Kashmir, Himachal Pradesh (HP), and Uttaranchal, *Angelica glauca* Edgew (Apiaceae), a high-value perennial medicinal herb endemic to the Indian Himalaya[1,2] is now endangered[3–5]. Locally known as 'Chora', it grows between 2000 and 3800 m altitudes in the Himalaya. For unique flavour and stimulating properties, local folk traditionally use its roots as a spice, in constipation and vomiting, and for its cardioactive, carminative and diaphoretic activities, yielding 1.3% essential oil[6]. Fruits are used in flavouring food items[7]. In recent years, high trade has threatened its natural populations. In 1999–2000, HP alone produced about 100 kg essential oil, 30% of which was exported (S. Mohan, pers. commun.). In addition, its natural populations in HP is very low (unpublished), which may be due to poor seed germination. Low seed germination in Apiaceae is known[8–10]. Using seeds of Uttaranchal population of *A. glauca*, Nautiyal *et al.*[9] reported only 8% maximum germination.

An experts' group prioritized *A. glauca* for conservation through *ex situ* cultivation for HP[4]. Enhancing seed germination and developing vigorous seedlings is crucial for this purpose. Pre-sowing chemical treatments have generally been used to enhance seed germination[10–15] and to increase seedling vigour[13,16,17]. The objectives of the present study include: (i) develop effective pre-sowing treatments to stimulate seed germination and seedling vigour and (ii) identify morphological traits for the assessment of healthy seedlings of *A. glauca*.

Seeds of *A. glauca* were collected in early October 2001 from moist, humus-rich riverine forests of upper Parvati valley, Kullu, HP (altitude 2500 m), dried for a week at room temperature (25 ± 2°C) and stored (4°C) before experimentation during the following April. Like many species of Apiaceae[18], seeds of *A. glauca* also experience heavy frost and very low winter temperatures in the wild. The fruits (schizocarp) consist of two one-seeded-mericarps that separate during ripening[19]; we refer to each mericarp as a seed. Thirty dried seeds were used to determine average fresh weight (8.0 ± 2.0 mg), dry weight (7.2 ± 1.8 mg), mean length (11.47 ± 1.12 mm), width (7.06 ± 0.97 mm) and thickness (1.06 ± 0.17 mm). Screening of 3000 seeds showed that 80% were healthy, 19% shrunk and 1% insect-damaged. Healthy seeds were used for all treatments. Thirty seeds were weighed and oven-dried at 80°C for 48 h. The moisture content was found to be 10%. Seed viability was observed both immediately after collection (67%) and at the time of germination tests (57%) using the tetrazolium test[20]. For germination tests, air-dried seeds were disinfected with 0.04% $HgCl_2$ (1 min), washed thoroughly with double distilled water (DW), and dipped in various pre-treatment solutions (24 h, 25 ± 2°C, dark). These include gibberelic acid (GA_3; 25 and 250 µM); 6-benzylaminopurine (BAP; 25, 100 and 250 µM, GA_3 25 µM + BAP 25 µM, GA_3 250 µM + BAP 250 µM, KNO_3 (50, 100 and 150 mM) and $NaHClO_3$ (5% available chlorine for 15, 30 and 45 min). Control was maintained using DW. Treated seeds were washed 2–3 times with DW and placed in petri dishes lined with Qualigens (615 Å) filter paper (three replicates/treatment, 50 seeds/replicate) in randomized design under laboratory conditions (average temperature: 29.02 ± 2.10°C max, 27.8 ± 2.20°C min) and monitored daily. The filter papers were moistened daily using DW. Seeds were considered germinated upon radicle emergence; the first germination was observed after

*For correspondence. (e-mail: badolahk@yahoo.co.in)